©*Operative Dentistry, 2021*, **46-6**, 650-660

Restoration of Severely Damaged Endodontically Treated Premolars: Influence of the Ferrule Effect on Marginal Integrity and Fracture Load of Resin Nano-ceramic CAD-CAM Endocrowns

GT Rocca • JJ Canneto • N Scotti • R Daher
A Feilzer • CM Saratti • I Krejci

Clinical Significance

Endocrowns are a valuable alternative to classical post-and-core crowns for the restoration of severely damaged premolars. The adjunction of a ferrule to the endocrown design does not seem to have an impact on its marginal integrity and load-bearing capacity.

SUMMARY

Objectives: To explore the ferrule effect on Resin Nano-Ceramic (RNC) premolar endocrown marginal integrity and fracture resistance.

Methods: Thirty-six root–canal-treated premolars were cut 2 mm above the cemento-enamel junction (CEJ). They were restored with standardized RNC computer-aided design/computer-aided manufacturing (CAD/CAM) restorations (Lava Ultimate, 3M Oral Care, St. Paul, MN, USA) and divided into three groups (n=12): endocrowns with a 3-mm endo-core (Group 1), endocrowns with a 3-mm endo-core and a 2-mm ferrule (Group 2), and

*Giovanni Tommaso Rocca, Department of Cariology and Endodontics, School of Dentistry, University of Geneva, Switzerland

Jean Jacques Canneto, DMD, Department of Cariology and Endodontics, School of Dentistry, University of Geneva, Switzerland

Nicola Scotti, DMD, Department of Cariology and Operative Dentistry, School of Dentistry, University of Turin, Italy

Rene Daher, DMD, Department of Cariology and Endodontics, School of Dentistry, University of Geneva, Switzerland

Albert Feilzer, professor, Department of Dental Materials, Academisch Centrum Tandheelkunde Amsterdam, Amsterdam, The Netherlands

Carlo Massimo Saratti, DMD, Department of Cariology and Endodontics, School of Dentistry, University of Geneva, Switzerland

Ivo Krejci, Professor, Department of Cariology and Endodontics, School of Dentistry, University of Geneva, Switzerland

*Corresponding author: 19 Rue Lombard, 1205 Geneva, Switzerland; E-mail: giovanni.rocca@unige.ch

http://doi.org/10.2341/20-081-L

conventional post-and-core crowns with a 2-mm ferrule (Group 3). All specimens were submitted to thermo-mechanical cycling loading (TMCL) (1.7 Hz, 49 N, 600 000 cycles, 1500 thermocycles). Margins were analyzed before and after the TMCL. In the second part of the experiment, the surviving specimens were submitted to unidirectional monotonic loading until fracture. Fragments were then analyzed using scanning electron microscopy (SEM) and the fracture mode was established.

Results: Endocrowns of Groups 1 and 2 performed better than conventional crowns (Group 3) in terms of marginal continuity. Differences in fracture load values within all groups were not statistically significant. Most of the specimens fractured in a non-repairable way.

Conclusions: The present test failed to provide evidence of any kind of difference between endocrowns with and without a ferrule in terms of load-bearing capacity and marginal integrity after fatigue. Further studies are needed to confirm the role of the ferrule in adhesive restorations of endodontically treated teeth.

INTRODUCTION

This research addresses the restoration of severely damaged endodontically treated premolars. The most common technique used for the reconstruction of extremely damaged teeth consists of fabricating a porcelain fused to metal (PFM) crown over an internal core which is built around a cemented radicular post. Today, restorative strategies based on adhesive techniques, such as direct composite resins and indirect CAD-CAM workpieces, are reliable alternatives to this classical approach.

Within the category of indirect restorations, endocrowns are becoming more and more popular in clinics. These are overlays made of monolithic ceramic or composite resin that restore the coronal portion of a root–canal-treated tooth by means of an extension inside the former pulp chamber called the endo-core. This extension provides stability and increases the adhesive surface, improving retention of the coronal part. Endocrowns present several advantages over classical crowns. For one thing, the absence of a deep anchoring in the root allows the preservation of more residual dentinal structure and reduces complications associated with long post placement such as root perforation or root fracture.[1,2] Moreover, the fabrication of a core inside an endocrown is not needed. This simplification of the clinical procedure is associated with reduced costs, especially for CAD/CAM restorations made chair-side.[3] In addition, endocrowns may present an easier obstacle when performing endodontic retreatments, as the restoration extends inside the root for a few millimeters, and no metal is included in the restoration. Nevertheless, concerns may arise when this kind of restoration breaks. The absence of a metallic substructure could leave subjacent tissues exposed to catastrophic vertical fracture.[4,5]

It is recognized that endodontically treated teeth (ETT) are more prone to fracture than vital ones.[6] The fracture resistance of ETT depends on many factors, such as the loading context, the type of restoration, and the quality and quantity of residual tissues.[7,8,9] The use of a ferrule as a reinforcing element in residual tissues is a widely debated issue.[10,11] The ferrule's mechanism of action relies on the protective role of the cervical part of the prosthetic crown that surrounds the residual tooth structure and acts as a ring that avoids the deflection of residual tissues and strengthens the tooth. Moreover, this strip of tissue improves the contact between the prosthetic crown and the rest of the root, thus enhancing its retention. According to classical prosthetic principles, the ferrule should be a minimum of 1 mm to 2 mm high, have parallel axial walls, encircle the tooth and end on sound tooth structure. In the scientific literature, many studies, the majority of which refer to conventional crown restorations, confirm the positive effect of a ferrule when restoring ETT.[4,12,13,14,15,16,17]

The favorable influence of a ferrule-integrating cavity beneath large, adhesive indirect restorations such as endocrowns for the restoration of devitalized teeth still needs to be proved. Few *in vitro* studies exist on this topic. Einhorn and others[4] showed that the addition of a ferrule into the cavity configuration of lithium disilicate molar endocrowns increased their fracture strength, with no difference in load-bearing resistance between preparations showing a 1 mm- or 2 mm-high ferrule in dentin. Similar findings were found by Taha and others[18] for polymer-infiltrated ceramic-network (PICN) molar endocrowns. Rocca and others[19] showed that when compared to classical post-and-core crown restorations, premolar endocrowns made of lithium disilicate-reinforced ceramic with butt margins (no ferrule) performed as well as conventional crowns (with ferrule) in terms of marginal integrity and resistance after fatigue.

The aim of this study was to investigate the influence of the "ferrule effect" on marginal adaptation, fracture resistance, and mode of fracture of RNC CAD/CAM premolar endocrowns. The integration of a ferrule into the endocrown cavity design was tested and compared to conventional crowns with post and core. Considering both the marginal adaptation (before and after cyclic stress) and load-bearing capacity of the restorations, it was hypothesized that a) the presence of the ferrule improves endocrown performance, and b) endocrowns perform better than crowns.

METHODS AND MATERIALS

Thirty-six recently extracted human upper premolars of approximately the same size were used in this study. The inclusion criteria were the absence of carious lesions and visible crack lines in the root and a complete root formation. Bucco-palatal and mesio-distal dimensions as well as the root length of each tooth were measured using a digital caliper. The teeth were then stored in a sodium azide solution (0.2%) at 4°C until the experiment onset.

Endodontic Procedure

All teeth were endodontically treated. The pulp chamber of each specimen was opened with diamond burs following a standardized procedure. Working length was determined visually by passing a #15 K-file (Dentsply Maillefer, Ballaigues, Switzerland) into the root canal until its tip was visible from the apical foramen. The root canal preparation was performed using nickel-titanium (NiTi) rotary instruments (ProTaper U, Dentsply) until the F3 instrument (ISO 30) in a low-speed handpiece (X-Smart, Dentsply) under intermittent rinsing with 4.2% sodium hypochlorite. All instrumentation was performed according to the manufacturer's instructions. A set of ProTaper U was replaced after the preparation of four canals. A resin-based endodontic sealer (AH Plus, Dentsply-DeTrey, Konstanz, Germany) and warm gutta-percha were inserted into the root with a vertical condensation technique (System B and Elements Obturation Unit gutta-percha extruder, Kerr Dental, Orange, CA, USA). Teeth were stored for 24 h in distilled water at 37°C before cavity preparation.

Cavity Preparation

Each specimen was placed on a metallic holder (Baltec, Balzer, Liechtenstein) and fixed in a vertical position by means of light-curing composite; the root base was then embedded with self-curing acrylic resin up to 1 mm below the cemento-enamel junction (CEJ) to obtain full stabilization of the teeth. The crown of each tooth was horizontally sectioned with a diamond disk (Kerr Dental, Brea, California) 2 mm occlusal to the CEJ. The teeth were then randomly assigned to three groups (n=12). In Group 1, coronal tissues were horizontally cut at the CEJ, and gutta-percha was removed from the pulp chamber until 3 mm below the CEJ. For Group 2 and 3 specimens, a peripheral chamfer (1 mm wide, 2 mm high) was integrated to create a ferrule effect, and gutta-percha was removed as in Group 1. In all prepared teeth, mesio-distal and bucco-palatal dimensions were measured with a digital caliper 3.3 mm ± 0.2 mm and 6.5 mm ± 0.2 mm respectively. All procedures were performed using coarse diamond-coated burs (Cerinlay No. 3080.018 FG, Intensiv, Viganello, Switzerland) and finished with fine-grained burs of the same shape (Cerinlay No. 3025.018 FG, Intensiv) under abundant water spray cooling. All cavity dentin surfaces were sealed with a self-etch adhesive system (Scotchbond Universal Adhesive, 3M Oral Care) according to the manufacturer's recommendations. The bonding resin was polymerized for 20 seconds with a second-generation LED high-power device (Bluephase, Ivoclar Vivadent, Schaan, Liechtenstein) which delivered a power density of 1200 mW/cm^2. After the immediate dentin-sealing procedure, for Groups 1 and 2, digital impressions were made (Cerec Omnicam, Dentsply Sirona, York, PA, USA). Then the cavities were coated with a water-based glycerine gel (Airblock, Dentsply), and teeth were provisionally restored with a soft light-curing resin (Fermit N, Ivoclar Vivadent) and kept in saline solution for 7 days at 32°C. For Group 3, a pre-calibrated glass-fiber post (RelyX Fiber Post, 3M Oral Care) was inserted into the palatal canal for a length of 5 mm and luted with universal dual-curing resin cement (RelyX Ultimate, 3M Oral Care) following the manufacturer's recommendations. Then a 3.5-mm-high core was fabricated with a restorative nano-hybrid composite resin (Filtek Supreme XTE Universal Restorative, A2 shade, 3M Oral Care); digital impressions were made (Cerec Omnicam, Dentsply) and teeth were provisionally restored as for Groups 1 and 2.

Fabrication of the Restorations

The prepared premolars were divided into three groups and restored with RNC CAD/CAM material (Lava Ultimate, 3M Oral Care) as follows (n=12):

- Group 1: CAD/CAM RNC endocrowns with a 3-mm integrated endo-core.
- Group 2: CAD/CAM RNC endocrowns with a 2-mm integrated ferrule and 3-mm integrated endo-core.
- Group 3: CAD-CAM RNC post-and-core crowns with a 2-mm integrated ferrule.

A schematic representation of the experimental design of this study is shown in Figure 1.

All restorations were created with nearly identical

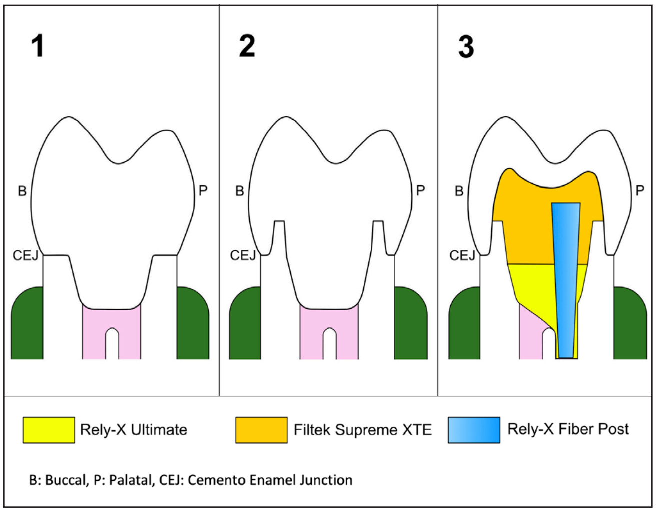

Figure 1. *Experimental design of the study. Group 1 and 2 restorations were 5.5-mm thick from the mesio-distal sulcus to the cemento-enamel junction (CEJ) (without considering the 3-mm high endo-core for Groups 1 and 2). Group 3 crowns had a thickness of 2 mm from the mesio-distal sulcus to the resin core. The inner core of Group 3 specimens was 3.5-mm high from the CEJ including 2 mm of ferrule.*

dimensions and with the same cusp occlusal angle, using one of the intact extracted maxillary first premolars as a master model in Cerec 4.0 software in Biogeneric Copy Design Mode.

Luting Procedures

Lined cavities of Groups 1 and 2, the core preparations of Group 3 and the intaglio surfaces of all the restorations were submitted to airborne-particle abrasion with 27 µm aluminium oxide particles at about 0.2 MPa pressure for 5 seconds (Kavo EWL, Type 5423, Biberach, Germany), then rinsed and dried. The self-etch adhesive system (Scotchbond Universal Adhesive, 3M Oral Care) was applied on all prepared surfaces prior to cementation following the manufacturer's instructions. The bonding resin was left uncured, and the restoration was placed in a box, protected from light (Vivapad, Ivoclar Vivadent) until cementation. The tooth preparations were covered with a thin layer of dual-curing resin cement (RelyX Ultimate, 3M Oral Care) before seating the restoration. The restoration was placed first with manual pressure and then with the assistance of a specific ultrasonic device (Cementation Tip, EMS, Nyon, Switzerland). The plastic-coated ultrasonic tip was activated at the center of the restorative surface for 3 seconds to seat the workpiece into definitive position. After removal of excess cement, the restoration buccal, occlusal, and lingual surfaces were light cured for 90 seconds separately. Restorations were then immediately finished and polished, using flame- and pear-shaped fine diamond burs (40 µm, then 25 µm grain size) (Intensiv Nos. 4205L, 4255, 5205L and 5255, Intensiv), and discs of decreasing grain size (Pop-On XT, 3M Oral Care) were used to polish their margins.

A summary of the products used in this study is listed in Table 1.

Thermo-mechanical Fatigue Loading

The stress test was carried out 24 hours after cementation in a chewing simulator (Chewing simulator CS-4, SD Mechatronik, Feldkirchen-Westerham, Germany) for TMCL. All specimens were subjected to 600,000 cycles with a 49 newton (N) eccentric occlusal loading force on the inner side of the buccal cusp. The force was applied with a metallic ball of 4 mm in diameter at 1.7 Hz frequency following a one-half sine wave curve. By having the specimen holder mounted on a hard rubber disc, a sliding movement of the tooth was produced between the first contact on an inclined plane of the buccal cusp and the central fossa (Figure 2). A total of 3000 thermocycles at 5°C to 50°C to 5°C were performed simultaneously.

Marginal Analysis

Before the fatigue test, as well as after completion of the loading phase, gold-sputtered epoxy resin replicas (Epofix, Struers, Rødrove, Denmark) were made from polyvinylsiloxane impressions (President light, Coltène, Altstätten, Switzerland). The dentin margins on the proximal side, below the CEJ, were observed. The tooth–cement interface (TC) was analyzed semiquantitatively by scanning electron microscopy (SEM) (Digital SEM XL20, Philips, Eindhoven, Netherlands), employing an established evaluation method. The margins were evaluated at a standard 200× magnification; when required for assessment accuracy, higher magnifications up to 1000× were used. The following evaluation criteria were considered: perfect adaptation (continuity), underfilling, overfilling, marginal opening, and tooth or restoration fracture. Results for marginal adaptation before and after the loading phase are expressed as percentages of "perfect adaptation" (defect-free). Percentages were calculated as the ratio between the cumulative distance of all segments showing the same morphological quality and the whole interface length.

Fracture Test

After fatigue, all groups were subjected to fracture load evaluation in a universal testing machine (Dyna-Mess, Stolberg, Germany) according to an established method. Each specimen was placed in

Table 1: *Summary of Materials Used*

Material	Brand Name	Chemical Composition	Elastic Modulus	Batch Number
Adhesive system	Scotchbond Universal Adhesive (3M-ESPE)	MDP, dimethacrylate, HEMA, Vitrebond copolymer, filler, ethanol, water, initiators and silane		T02489
Resin cement	Rely-x Ultimate (3M-ESPE)	Base paste: methacrylate monomers, silanated fillers, initiators and stabilizers Catalyst paste: methacrylate monomers, fillers, pigments, initiators and stabilizers	7.7 GPa	T03823
Fiber glass post	Rely-x fiber post (3M-ESPE)	Glass fibers, composite resin	36 GPa	S14125
Composite resin	Filtek Supreme XTE Universal Restorative (3M-ESPE)	Methacrylates, fillers, initiators and stabilizers	10 GPa	S45474
RNC blocks	Lava Ultimate (3M-ESPE)	Highly cross-linked resin matrix reinforced by 80% by weight of silane treated nano zirconia-silica particles agglomerated to clusters (0.6-10 μm) and individual silane bonded nano silica or zirconia particles (< 20 nm)	15 GPa	S58320
Temporary resin	Fermit N (Ivoclar-Vivadent)	Methacrylates, dispersed silicon dioxide and copolymers, catalysts and stabilizers		S45172

Abbreviations: GPa, gigapascal; HEMA, 2-hydroxyethyl methacrylate; μm, micrometer; nm, nanometer.

a fixing device, and a controlled load was applied axially to the longitudinal axis of the root, using a stainless steel rod (diameter 5 mm). Pressure on the tip was applied in the middle of the occlusal surface at a crosshead speed of 1 mm/minute. Specimens were loaded until fracture and the maximum breaking loads were recorded in Newtons (N). The modes of fracture were analyzed by optical stereomicroscopy and classified as repairable restoration fracture, above the CEJ (type A), non-repairable/catastrophic vertical fracture, inside the restoration, below the CEJ (type B) and root fracture not involving the restoration (type C). Fractographic analysis by means of SEM was performed on selected specimens. To remove all the impurities, all fragments were cleaned in an ultrasonic 10% sodium hypochlorite bath for 3 minutes, rinsed with water, dried, and then fixed on the support for the microscope. The specimens were gold coated prior to the analysis with the SEM. Magnifications up to 2000× were used to obtain higher definition of identified crack features in selected areas of interest. The overall direction of crack propagation and failure origin(s) were systematically mapped for all specimens.

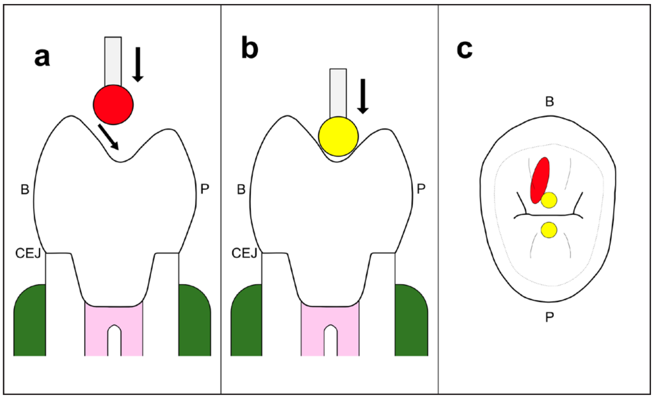

Figure 2. *Schematic representation of (a) the sliding action of the ball indenter over the buccal cusp of the specimen during the Thermo-Mechanical Cycling Loading (TMCL test) and (b) the monocycle stress test. In the occlusal view (c), the contact of the sliding movement is in red and the contact points of the fracture strength test are in yellow.*

Statistics

Marginal Adaptation

Data and statistical analyses were elaborated with R software, version 2.15.2 (R Foundation for Statistical Computing, Wien, Austria). The primary outcome was marginal adaptation, while the tested independent factors were the TMCL test (before and after fatigue) and the restoration technique (Groups 1 to 3). Because of the low specimen quantity in each group (n=12) and the uneven distribution of the primary outcome data, differences in marginal adaptation before and after stress were assessed by means of paired Wilcoxon tests. For the same reasons, differences in marginal adaptation between the techniques were estimated using Kruskal-Wallis tests. In the case of significant differences in marginal adaptation between the techniques, *post hoc* tests were used for pairwise multiple comparisons applying the Nemenyi test. To investigate the ferrule effect inside endocrowns, Group 1 data were compared to those of Group 2 (hypothesis a). For the comparison between endocrowns and crowns, the results of Groups 1 and 2 were paired and compared to those of Group 3 (hypothesis b). For all analysis, alpha level was set at 0.05.

Fracture Resistance

A Kruskal-Wallis test ($p>0.05$) was applied to assess the differences between the groups. Comparisons of the fracture load values of specimens were also achieved via Kaplan-Meier product limit estimation (OriginPro 8). Kaplan-Meier product limit estimation and fracture load values were established separately for the three groups. Plots of survival distribution were obtained for each group. The log rank method was used as test of the equivalence of survival times across groups. For the three groups, percentiles of the survival function (with lower and upper confidence limits) were calculated. The influence of the ferrule for endocrowns was assessed by comparing results of Group 1 and Group 2 (hypothesis a). The comparison between endocrowns and crowns (hypothesis b) was investigated by pairing results of Group 1 and Group 2 and comparing them to those of Group 3.

RESULTS

Marginal Adaptation

All the tested specimens survived the TMCL test. For each specimen, the percentage of perfect margin adaptation was calculated before and after the fatigue test. The results and statistical analysis are shown in Table 2 and Figure 3.

For all specimens, the results of perfect margin adaptation after stress were significantly lower than before loading. There was a significant difference between the experimental techniques in both before and after fatigue values. The highest median values were recorded for Groups 1 and 2, while Group 3 showed the lowest values. Groups 1 and 3 displayed the greatest difference of values for closed margins before and after the stress.

Integration of a ferrule (Group 2) into the classical endocrown design (Group 1) did not have any effect on marginal adaptation of the restorations.

Considering pairwise analysis of factors, endocrowns of Groups 1 and 2 performed better than crowns of Group 3 before and after stress even though degradation of the margins following the TMCL test was equivalent.

Fracture Resistance

The fracture load results are shown in Table 3. No significant differences were found between the groups with the Kruskal-Wallis test ($p>0.05$). Also, analysis of the Kaplan-Meier-plotted survival curves did not show any significant differences between the three groups (Figure 4). According to the Kruskal-Wallis test, the presence of a ferrule did not improve the load-bearing

Table 2: *Results of Marginal Analysis Expressed as Median and Interquartile Percentage Ranges of Perfect Adaptation for the Three Groups (n=12), Before and After Loading*

Group	Before[a]	After[a]	Diff (Af–Be)	p-value[c]
1	97 [94; 100] (3)	87 [79; 89] (3)	-12 [-16; -6]	<0.001
2	97 [94; 99] (3)	91 [85; 93] (3)	-5 [-8; -3]	<0.001
3	79 [73; 87] (1,2)	66 [60; 69] (1,2)	-13 [-25; -8]	<0.001
p-value	<0.001[b]	<0.001[b]	0.059[b]	

[a]*Data are medians [25th percentile; 75th percentile]. Numbers in parentheses represent the group(s) with which the concerned group is different according to the Nemenyi test.*
[b]*Kruskal-Wallis test.*
[c]*Wilcoxon paired test.*

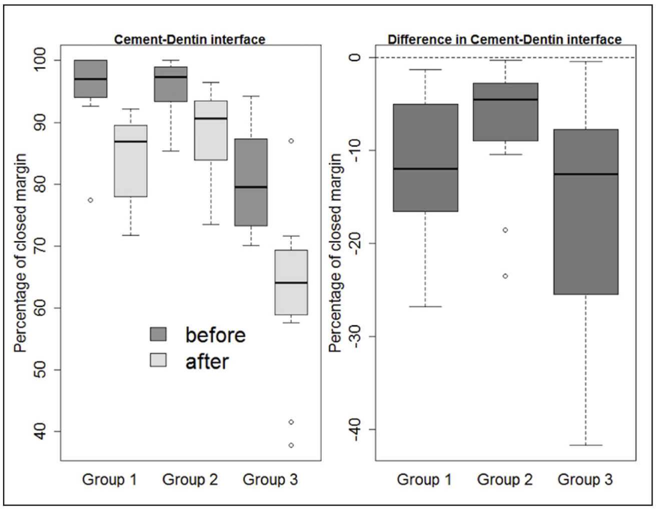

Figure 3. *Box-and-whisker plots indicating percentages of "closed margins" for the three groups, before and after thermo-mechanical cycling loading (TMCL) fatigue loading.*

capacity of the specimens of Group 2 compared to those of Group 1. Pairwise comparison of endocrowns and crowns did not show any difference in fracture resistance. The modes of failure are shown in Table 4. Most of the specimens experienced non-repairable fractures of type B, with a vertical fracture pattern which originated at the occlusal surface and progressed in an apical direction, splitting the restoration and the tooth mesio-distally (Fig. 5). As revealed by stereomicroscopic analysis, the fracture originated in all these cases under the loading area of the metallic indenter. However, some specimens of Group 3 (30%) fractured favourably, above the CEJ (type A fractures) (Figure 5). In all groups, a small percentage of restorations survived the test because of horizontal root fractures that left intact the tooth–restoration interface (type C fractures).

Table 3: *Fracture Strength Test Results Expressed as Mean Fracture Loads and Standard Deviations, Median and Interquartile Values and Ranges*

		Fracture Load (N)		
Group	**n**	**Mean ± SD**	**Median (IQ)**	**Range**
1	12	894 ± 228	912 (699 - 1046)	444 to 1213
2	12	851 ± 145	845 (799 - 911)	568 to 1100
3	12	948 ± 318	1014 (782 - 1158)	386 to 1320
p-value		0.626[a]	0.317[b]	—

Abbreviations: IQ, interquartile; N, newton; SD, standard deviation.
[a]*Linear regression model*
[b]*Kruskal-Wallis test*

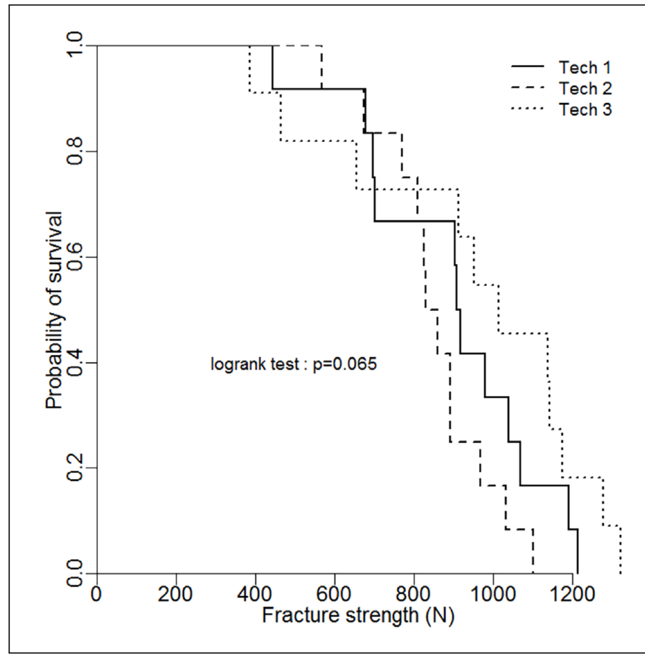

Figure 4. *Kaplan–Meier plotted survival curves for the three groups.*

DISCUSSION

In the present study, the investigators evaluated the impact of a ferrule on the marginal adaptation and fracture load of premolar endocrowns. To the best of the authors' knowledge, few studies exist on this topic. Results showed that the presence of a ferrule did not have any influence, either on marginal adaptation or on fracture resistance within the different endocrown restorations, meaning that hypothesis a was rejected.

Endocrowns performed better than crowns in terms of marginal integrity after cyclic stress, but their load-bearing resistance to the following monotonic loading was equivalent. Thus, hypothesis b was partially accepted. Severely destroyed first upper premolars were employed as specimens for this test because the efficacy of endocrowns to restore endodontically treated premolars still needs to be proved.[20] The worst clinical scenario was simulated by cutting the teeth at the CEJ and eliminating all of the anatomical crown. An endo-core length of 3 mm was chosen because it has been previously demonstrated that an extension of 3 mm inside the pulp chamber is sufficient to assure good marginal integrity and resistance to fatigue of premolar restorations.[19,21]

An extracted upper premolar was used as the master model for crown shape and dimension of all milled restorations. An RNC CAD/CAM material (Lava Ultimate) was used for the restorations, because it is

Table 4: *Types of Macroscopic Failure for the Three Groups*

Fracture Mode	Group 1 (#)	Group 2 (#)	Group 3 (#)
Type A 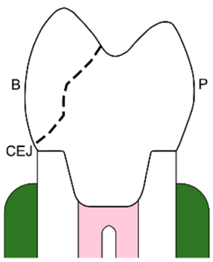	0	0	4
Type B 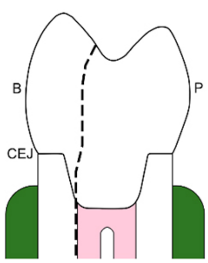	10	9	6

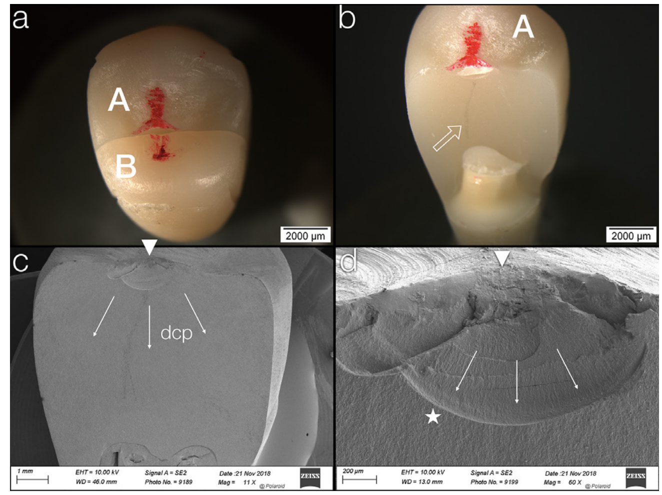

Figure 5. *A typical type B catastrophic fracture. (a) Occlusal view from the stereomicroscope of the fractured specimen after repositioning of the two main halves. The red mark on the occlusal surface indicates the contact loading area of the monotonic strength test. (b) View of the fractured surface of fragment A. The crack started from the occlusal surface in a corono-apical direction and ended inside the root of the tooth with a smooth surface (fast fracture), causing the specimen to split. (c) Scanning electron micrograph (SEM) large view of the fractured surface. The white tip indicates the primary crack origin. Hackle lines on the surface indicate the direction of crack propagation (dcp, white arrows). (d) Details of the primary crack origin at higher magnification. Hackle lines are clearly visible.*

among the most commonly used materials in the chairside fabrication of indirect restorations.

Specimens were fatigued by TMCL in a chewing simulator. A chewing force of 49 N was applied for 600,000 cycles at 1.7 Hz to reproduce *in vivo* masticatory conditions corresponding to approximately 2.5 years of clinical function in the premolar region.[5,22,23] The sliding movement produced by the design of this test induced shearing stresses at the tooth-restoration interface, reproducing the effect of premolar guidance during the eccentric movements and exacerbating the testing conditions.[24] No artificial periodontium was employed around the roots, as materials used for this purpose tend to degrade and deform during the test and are therefore not standardizable. This could have negatively influenced the results of this test, as the periodontal ligament is a physiological shock absorber that plays a non-negligible role in *in vivo* conditions.[19,25] Evaluation of the marginal adaptation of restorations was performed before and after the TMCL test. As expected, fatigue had a negative effect on marginal integrity for all specimens. In fact, it is well known that aqueous media, mechanical cyclic loading, and thermal stresses have a degrading effect on resin-bonded interfaces.[26-30]

The results of this study indicate that endocrowns of both Groups 1 and 2 performed better than crowns of Group 3 in terms of marginal integrity both before and after fatigue. This difference in outcomes even before the fatigue stress—just after polishing of the specimens' margins—was not expected, as materials and luting conditions were the same for all specimens. The different geometry of the workpiece may have induced greater polymerization contraction stress at crown restoration margins compared to the endocrown interfaces, resulting in a lower quality of marginal adaptation. Further studies are necessary to confirm this hypothesis, as these results are in contrast with the trends observed in previous *in vitro* studies.[19,31] In this study, degradation of margins (the difference between before- and after-fatigue values) was the same for all specimens, meaning that the technique used for restorations did not have an impact on the ageing of the adhesive interface.

All specimens survived the TMCL test. In the second part of the experiment, the specimens were stressed with a unidirectional monotonic load until fracture.

Results of Kruskal-Wallis tests and Kaplan-Meyer survival curves displayed no significant differences for maximum static breaking loads among all three kinds of restored premolars. The similarity in the results within RNC endocrowns of Groups 1 and 2 (5.5 mm thick) and RNC crowns of Group 3 (2 mm thick) was expected despite the large discrepancy in the thickness of the restorations. In a previous study conducted by Chen and others,[32] there was also no linear relation between fracture resistance and the thickness of RNC restorations. These results are also consistent with the outcomes of studies by Ramírez-Sebastià and others[33] and Rocca and others.[5] Likewise, the fracture load test failed to provide evidence of any difference between endocrowns with and without a ferrule in the cavity preparation design. The importance of the thickness of the RNC endocrowns and the high loads needed to break them could explain the lack of effect of the two different preparations. It is reasonable to suppose that the similar mean load-bearing ability described for Groups 1 and 2 specimens reflects principally the final strength of the thick restoration more than the different cavity design. These results are not in agreement with previous *in vitro* studies in which ceramic molar endocrowns with ferrules outperformed those without them.[4,18] Further *in vitro* studies are needed to clarify this issue.

In June 2015, 3M Oral Care removed the crown (and even endocrown) indication for its LAVA Ultimate CAD-CAM restorative product because of a higher-than-anticipated rate of debonding, while leaving the indication for inlays/onlays and veneers. In that notice, no details were included about the type of crowns involved (anterior vs posterior crowns, thickness of restoration), material of the core, or, above all, about the adhesive strategy involved in the debonded cases (type of cement, surfaces pre-treatment).[5] In the present study, this product demonstrated good adhesive behavior in terms of marginal integrity after fatigue of both LAVA crowns and endocrowns, without any final debonding. Magne and others[34] had previously investigated fatigue behavior after accelerated fatigue testing (stepwise loading) of molar crowns (2.5 mm and 1.5 mm thick) and endocrowns (3.5 mm thick) fabricated with the same RNC material and bonded to dentin and composite cores. No ferrule was included in the tooth cavity design. All restorations survived the normal ranges of posterior masticatory forces without any debonding. Later, the same group obtained similar good results in terms of adhesive and mechanical properties after fatigue for RNC molar crowns bonded to dentin, and their performances were equivalent to lithium-disilicate reinforced ceramic counterparts.[35,36] Several other *in vitro* studies showed excellent mechanical properties of RNC crowns and endocrowns bonded to resin dentin analogues.[5,37,38] To the best of the authors' knowledge, no clinical trials exist at present that evaluate LAVA Ultimate crowns bonded to natural tissues or conventional composite resin cores. A recent randomized clinical trial on posterior implants restored with zirconia abutments and RNC crowns encountered a high rate (80%) of premature bonding failure, discouraging the use of this material for crowns bonded to rigid zirconia abutments.[39]

With regard to the mode of fracture, almost all specimens fractured in a catastrophic way (type B fracture) because of vertical restoration-root fractures (Figure 6). In these cases, stereomicroscopic analysis of the fractured specimens revealed that the origin of the primary crack was always placed under the main occlusal contact area of the loading ball indenter. The crack front propagates in a vertical corono-apical direction without obstacles and creating smooth fractured surfaces. Nonetheless, some Group 3 crowns showed more favorable fracture patterns. Fractographic analysis showed that in these cases the crack was deviated during its run at the adhesive interface between the crown and the core (Figure 5).

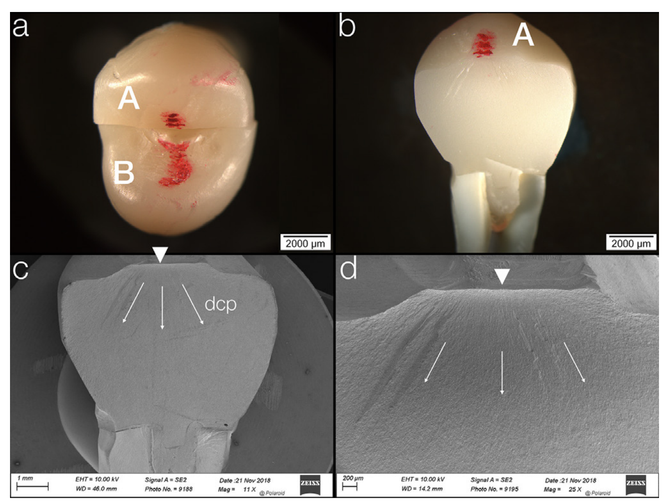

Figure 6. *An example of type A fracture of a crown. (a) Occlusal view from the stereomicroscope of the fractured specimen after repositioning of the two main halves. The red mark on the occlusal surface indicates the contact loading area of the fracture strength test. (b) Fracture started from the occlusal surface and had a corono-apical direction. The empty arrow indicates the trail of the metallic ball after the crack occurred. A deviation of the crack happened at the adhesive interface between the crown and the core. The fracture broke a portion of the resin core and then passed through the interface between the crown and the tissues of the core. These fractures were classified as repairable. (c) SEM large view of the fractured surface. The big white tip indicates the primary crack origin. White arrows indicate the direction of crack propagation, (dcp, hackle lines). (d) Details of the primary crack origin at higher magnification. The white star indicates an arrest line.*

CONCLUSIONS

Under the conditions of this *in vitro* study, RNC endocrowns that included a ferrule in the geometry of the cavity did not show better marginal adaptation after fatigue or improved fracture resistance after monotonic loading than endocrowns without a ferrule. Almost all specimens fractured in a catastrophic way, under the CEJ. Further *in vitro* studies and clinical trials are needed to confirm these results.

Acknowledgements

The Authors wish to thank 3M Oral Care for their kind supply of the tested materials. They would also like to thank Dr Antoine Poncet (CRC & Division of Clinical Epidemiology, Department of Health and Community Medicine, University of Geneva) for the statistical analysis and Dr Nicolas Rizcalla for the graphic support. This work was supported by the Swiss Dental Association (SSO), grant number 296-17.

Regulatory Statement

This study was conducted in accordance with all the provisions of the human subjects oversight committee guidelines and policies of Commission cantonale d'éthique de la recherche (CCER) in Geneva Switzerland.

Conflict of Interest

The authors have no financial interest in any of the companies or products mentioned in this article.

(Accepted 21 December 2020)

REFERENCES

1. Zicari F, Van Meerbeek B, Scotti R, & Naert I (2012) Effect of fibre post length and text adhesive strategy on fracture resistance of endodontically treated teeth after fatigue loading *Journal of Dentistry* **40(4)** 312–321.
2. Hatta M, Shinya A, Vallittu PK, Shinya A, & Lassila LV (2011) High volume individual fibre post versus low volume fibre post: The fracture load of the restored tooth *Journal of Dentistry* **39(1)** 65–71.
3. Tay FR & Pashley DH (2007) Monoblocks in root canals: Ahypothetical or a tangible goal *Journal of Endodontics* **33(4)** 391–398.
4. Einhorn M, DuVall N, Wajdowicz M, Brewster J, & Roberts H (2019) Preparation ferrule design effect on endocrown failure resistance *Journal of Prosthodontics* **28(1)** e237–e242.
5. Rocca GT, Sedlakova P, Saratti CM, Sedlacek R, Gregor L, Rizcalla N, Feilzer AJ, & Krejci I (2016) Fatigue behavior of resin-modified monolithic CAD-CAM RNC crowns and endocrowns *Dental Materials* **32(12)** 338–350.
6. Caplan DJ, Cai J, Yin G, & White BA (2005) Root canal filled versus non-root canal filled teeth: a retrospective comparison of survival times *Journal of Public Health Dentistry* **65(2)** 90–96.
7. Dietschi D, Duc O, Krejci I, & Sadan A (2008) Biomechanical considerations for the restoration of endodontically treated teeth: A systematic review of the literature, part II (Evaluation of fatigue behavior, interfaces, and in vivo studies) *Quintessence* **39(2)** 117–129.
8. Schwartz RS & Robbins JW (2004) Post placement and restoration of endodontically treated teeth: a literature review *Journal of Endodontics* **30(5)** 289–301.
9. Al-Omiri MK, Mahmoud AA, Rayyan MR, & Abu-Hammad O (2010) Fracture resistance of teeth restored with post-retained restorations: An overview *Journal of Endodontics* **36(9)** 1439–1449.
10. Kim AR, Lim HP, Yang HS, & Park SW (2017) Effect of ferrule on the fracture resistance of mandibular premolars with prefabricated posts and cores *Journal of Advanced Prosthodontics* **9(5)** 328–334.
11. Samran A, El Bahra S, & Kern M (2013) The influence of substance loss and ferrule height on the fracture resistance of endodontically treated premolars. An in vitro study *Dental Materials* **29(12)** 1280–1286.
12. Jotkowitz A & Samet N (2010) Rethinking ferrule—A new approach to an old dilemma *Brazilian Dental Journal* **209(1)** 25–33.
13. Clark D & Khademi J (2010) Modern molar endodontic access and directed dentin conservation *Dental Clinics of North America* **54(2)** 249–273.
14. Isidor F, Brøndum K, & Ravnholt G (1999) The influence of post length and crown ferrule length on the resistance to cyclic loading of bovine teeth with prefabricated titanium posts *International Journal of Prosthodontics* **12(1)** 78–82.
15. Libman WJ & Nicholls JI (1995) Load fatigue of teeth restored with cast posts and cores and complete crowns *International Journal of Prosthodontics* **8(2)** 155–161.
16. Stankiewicz NR & Wilson PR (2002) The ferrule effect: A literature review *International Endodontic Journal* **35(7)** 575–581.
17. Akkayan B (2004) An in vitro study evaluating the effect of ferrule length on fracture resistance of endodontically treated teeth restored with fiber-reinforced and zirconia dowel systems *Journal of Prosthetic Dentistry* **92(2)** 155–162.
18. Taha D, Spintzyk S, Schille C, Sabet A, Wahsh M, Salah T, & Geis-Gerstorfer J (2018) Fracture resistance and failure modes of polymer infiltrated ceramic endocrown restorations with variations in margin design and occlusal thickness *Journal of Prosthodontic Research* **62(3)** 293–297.
19. Rocca GT, Daher R, Saratti CM, Sedlacek R, Suchy T, Feilzer AJ, & Krejci I (2018) Restoration of severely damaged endodontically treated premolars: The influence of the endo-core length on marginal integrity and fatigue resistance of lithium disilicate CAD-CAM ceramic endocrowns *Journal of Dentistry* **68** 41–50.
20. Belleflamme MM, Geerts SO, Louwette MM, Grenade CF, Vanheusden AJ, & Mainjot AK (2017) No post-no core approach to restore severely damaged posterior teeth: an up to 10-year retrospective study of documented endocrown cases *Journal of Dentistry* **63** 1-7.
21. Lise DP, Van Ende A, De Munck J, Umeda Suzuki TY, Cardoso Vieira LC, & Van Meerbeek B (2017) Biomechanical behavior of endodontically treated premolars using different preparation designs and CAD/CAM materials *Journal of Dentistry* **59** 54–61.

22. Krejci I, Lutz F, & Krejci D (1988) The influence of different base materials on marginal adaptation and wear of conventional class II composite resin restorations *Quintessence International Journal* **19(3)** 191–198.

23. Kumagai H, Suzuki T, Hamada T, Sondang P, Fujitani M, & Nikawa H (1999) Occlusal force distribution on the dental arch during various levels of clenching *Journal of Oral Rehabilitation* **26(12)** 932–935.

24. Gresnigt MM, Ozcan M, van den Houten ML, Schipper L, & Cune MS (2016) Fracture strength, failure type and Weibull characteristics of lithium disilicate and multiphase resin composite endocrowns under axial and lateral forces *Dental Materials* **32(5)** 607–614.

25. Soares CJ, Pizi EC, Fonseca RB, & Martins LR (2005) Influence of root embedment material and periodontal ligament simulation on fracture resistance tests *Brazilian Oral Research* **19(1)** 11–16.

26. De Munck J, Van Landuyt K, Peumans M, Poitevin A, Lambrechts P, Braem M, & Van Meerbeek B (2005) A critical review of the durability of adhesion to tooth tissue: Methods and results *Journal of Dental Research* **84(2)** 118–132.

27. Nagai T, Kawamoto Y, Kakehashi Y, & Matsumura H (2005) Adhesive bonding of a lithium disilicate ceramic material with resin-based luting agents *Journal of Oral Rehabilitation* **32(8)** 598–605.

28. Rocca GT, Saratti CM, Poncet A, Feilzer AJ, & Krejci I (2016) The influence of FRCs reinforcement on marginal adaptation of CAD/CAM composite resin endocrowns after simulated fatigue loading *Odontology* **104(2)** 220–232.

29. Frankenberger R, Kramer N, Lohbauer U, Nikolaenko SA, & Reich SM (2007) Marginal integrity: Is the clinical performance of bonded restorations predictable in vitro? *Journal of Adhesive Dentistry* 9 **(Supplement 1)** 107–116.

30. Heintze SD (2013) Clinical relevance of tests on bond strength, microleakage and marginal adaptation *Dental Materials* **29(1)** 59–84.

31. Ramírez-Sebastià A, Bortolotto T, Roig M, & Krejci I (2013) Composite vs ceramic computer-aided design/computer-assisted manufacturing crowns in endodontically treated teeth: analysis of marginal adaptation *Operative Dentistry* **38(6)** 663–673.

32. Chen C, Trindade FZ, de Jager N, Kleverlaan CJ, & Feilzer AJ (2014) The fracture resistance of a CAD/CAM Resin Nano Ceramic (RNC) and a CAD ceramic at different thicknesses *Dental Materials* **30(9)** 954–962.

33. Ramírez-Sebastià A, Bortolotto T, Cattani-Lorente M, Giner L, Roig M, & Krejci I (2014) Adhesive restoration of anterior endodontically treated teeth: influence of post length on fracture strength *Clinical Oral Investigations* **18(2)** 545–555.

34. Magne P, Carvalho AO, Bruzi G, Anderson RE, Maia HP, & Giannini M (2014) Influence of no-ferrule and no-post buildup design on the fatigue resistance of endodontically treated molars restored with resin nanoceramic CAD/CAM crowns *Operative Dentistry* **39(6)** 595-602.

35. Magne P, Carvalho AO, Bruzi G, & Giannini M (2015) Fatigue resistance of ultrathin CAD/CAM complete crowns with a simplified cementation process *Journal of Prosthetic Dentistry* **114(4)** 574-579.

36. Carvalho AO, Bruzi G, Giannini M, & Magne P (2014) Fatigue resistance of CAD/CAM complete crowns with a simplified cementation process *Journal of Prosthetic Dentistry* **111(4)** 310-317.

37. Shembish FA, Tong H, Kaizer M, Janal MN, Thompson VP, Opdam NJ, & Zang Y (2016) Fatigue resistance of CAD/CAM resin composite molar crowns *Dental Materials* **32(4)** 499-509.

38. Zimmermann M, Ender A, Egli G, Özcan M, & Mehl A (2019) Fracture load of CAD/CAM-fabricated and 3D-printed composite crowns as a function of material thickness *Clinical Oral Investigations* **23(6)** 2777–2784.

39. Schepke U, Meijer HJ, Vermeulen KM, Raghoebar GM, & Cune MS (2016) Clinical bonding of resin nano ceramic restorations to zirconia abutments: A case series within a randomized clinical trial *Clinical Implant Dentistry and Related Research* **18(5)** 984-992.